

SIZE DETERMINATION OF NICKEL OXIDE NANOPARTICLES BY ELECTROCHEMICAL REDUCTION METHOD AND ITS ANTIBACTERIAL ACTIVITY

Ashwini A. Agale¹, Nitin R. Dighore², Sonali M. Janjal³, Suresh T. Gaikwad⁴,
Anjali S. Rajbhoj*⁵

Department of Chemistry, Dr. Babasaheb Ambedkar Marathwada University Aurangabad,
431004, (MS) India.

Article Received on
08 Oct 2015,

Revised on 29 Oct 2015,
Accepted on 18 Nov 2015

*Correspondence for
Author

Anjali Rajbhoj

Department of Chemistry,
Dr. Babasaheb Ambedkar
Marathwada University
Aurangabad,
431004, (MS) India.

ABSTRACT

Nickel oxide nanoparticles were synthesized by electrochemical reduction method using tetra butyl ammonium bromide (TBAB) and tetra octyl ammonium bromide (TOAB) as structure directing agents in an organic medium viz. tetra hydro furan (THF) and acetonitrile (ACN) in 1:4 ratio by optimizing current density 10mA/cm². The reduction process takes place over a period of 2 hrs. Such nanoparticles were prepared using simple electrolysis cell in which the sacrificial anode is commercially available nickel metal sheet and platinum (inert) sheet acts as a cathode. As the length of stabilizer increases the size of nanoparticles decreases. The parameters current density was also used to control the size of nanoparticles. The synthesized nickel oxide nanoparticles were characterized by FT-IR, UV, XRD, SEM-

EDS and TEM. Antibacterial activity of synthesized nanoparticles reveal that the nickel nanoparticles showed good antibacterial activity.

KEYWORDS: Electrochemical cell, Tetra octyl ammonium bromide, Tetra butyl ammonium bromide, nickel oxide nanoparticles, antibacterial study.

INTRODUCTION

Nanoparticles are distinct materials with the entire or a part of the structure having submicron dimension, preferably in the range of 1-100 nm. Nanoparticles in general have different electronic, magnetic and chemical properties as compared to the property of the bulk material.^[1] The main reason for that is their large surface-to-volume ratio which results from

their small sizes. Nickel nanoparticles in particular have been used in chemical cells, fuel cells, for solar energy absorption, as catalysts^[2], as magnetic materials, etc.^[3, 4] The demand for nano-nickel material has risen with the rapid development of different telecommunication equipm. Ents.^[5] Shape and size have been identified to have close relationship with chemical and physical properties of nanoscale materials. Nickel oxides are potential for applications of electrode materials in super capacitors due to their high electrochemical reaction activity.^[6] Electro analysis is taking advantages from all the possibilities offered by nanomaterials easy to be detected by conventional electrochemical methods.^[7-10] Because of these properties nanoparticles have many important applications in catalysis, sensing and imaging Nickel oxide (NiO) is a very important material extensively used in catalysis, battery cathodes, gas sensors, electro chromic films and magnetic materials.^[11] This difference in properties is due to the different effects like as small size effect, surface effect, quantum size effect and macroscopic quantum tunnel effect as discussed elsewhere.^[12,13] In recent years, nickel oxide nanoparticles has attracted much interests due to its novel optical.^[14] potential application in catalyst^[15] gas sensors^[16], electrochemical films, photo electronic devices and so on as discussed elsewhere.^[17]

1] EXPERIMENTAL

Materials

All chemicals (up to 99.99% purity) tetra alkyl ammonium bromide salts, namely TOAB, TBAB and tetrahydrofuran (THF), acetonitrile (ACN) were purchased HPLC grade from Sigma Aldrich and Rankem chemicals and used as such. The sacrificial anode in the form of nickel sheet and platinum sheet as inert cathode having thickness 0.25 mm and purity 99.99% were purchased from Alfa Aesar.

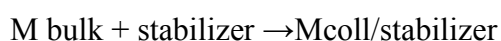
Method

Pure and size selective nanoparticles can be prepared by electrochemical method. This method was developed by Reetz.^[18,19] The process makes the use of an inexpensive two electrode set up for 25-30 ml electrolyte solution, which includes both oxidation of bulk metal and reduction of metal ions for size selective preparation of tetra alkyl ammonium salt stabilized metal nanoparticles. In the initial experiment we have used a nickel metal sheet (1x1 cm) as anode and a platinum sheet (1x1 cm) as the cathode. These two electrodes were placed parallel to one another and were separated by 1cm in 0.01 M solutions of tetra alkyl ammonium salt (TBAB) and (TOAB) were prepared in ACN/THF (4:1) served as the

supporting electrolyte. The electrolysis process was then carried out by applying current of $10\text{mA}/\text{cm}^2$ for 2 hrs. The nanoparticles thus formed were allowed to settle for one day. The agglomerated solid sample was separated from the solution by decantation and washed three to four times with THF. The washed samples were then dried under vacuum desiccators and calcinated at 600°C and used for characterizations.

Mechanism

During the synthesis, the bulk metal anode is oxidized and converted into metal cations. These cations migrate to the cathode and reduction takes place with the formation of metal in zero oxidation state.



Where, M bulk = metal bulk sheet,

M coll/stabilizer = ammonium salt stabilized colloidal metal cluster.

Lipophilic surfactants of the cationic type such as tetra alkyl ammonium halides ($\text{R}_4\text{N}^+\text{X}^-$) can give very stable NPs organosols.^[20] Quaternary ammonium compounds are a group of ammonium salts in which organic radicals are substituted for all four hydrogen of the original ammonium cation. They have a central nitrogen atom, which is joined to four organic radicals and one acid radical. The organic radicals may be alkyl or aryl and the nitrogen can be part of a ring system. They were prepared by treatment of an amine with an alkylating agent. They show a variety of physical, chemical and biological properties and most compounds are soluble in water and act as a strong electrolyte.

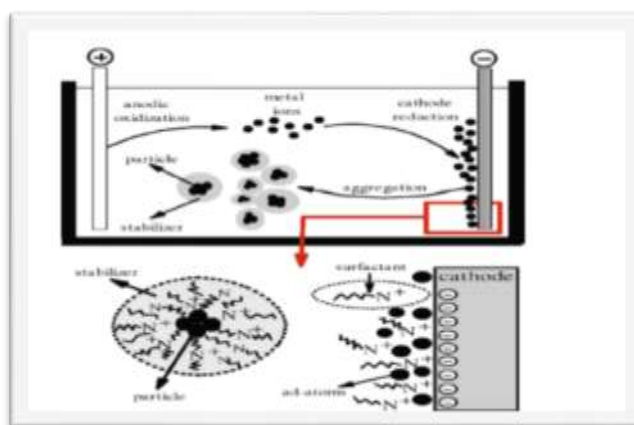


Fig: 1-(a).



Fig: 1-(b).

Fig: 1-(a) Mechanism of electrochemical reduction method and Fig: 1-(b) Black colored nickel NPs.

RESULT AND DISCUSSION

Characterization Techniques

The synthesized solid nanoclusters were mixed with KBr and FTIR spectra were recorded in the range of 400 to 4000 cm^{-1} on Jasco FTIR 8400 Spectrophotometer. In UV visible spectroscopic analysis supernatant of synthesized nanoparticles were used to record colour and study surface plasmon absorption in the UV-visible region using Jasco UV-Visible Spectroscopy. The powdered X-ray diffraction patterns were obtained out on X-ray powder diffractometer PW-1840, using $\text{CuK}\alpha$ radiation ($\lambda = 1.54 \text{ \AA}$). The samples were scanned from 20-820 at the scan rate of 5×10^4 CPS. The scanning electron microscopy study was carried out on JEOL make JSM 63608A microscope to study the morphology of the synthesized nanoparticles.

Transmission Electron Microscopy of synthesized nanoclusters were ultrasonicated in ethanol and then a drop of the dispersed nanoparticles was placed onto a carbon coated 400 mesh copper grid with format coating over it, followed by natural evaporation. Transmission electron microscopic study and electron diffraction were carried out on Philips CM 200kv.

1] Fourier Transform Infra-red studies (FTIR)

The FTIR spectrum of Ni/NiO NPs synthesized by using TBAB and TOAB capping agent and calcinated at 600°C. There is no peak indicating the presence of C-H stretching or

unconjugated C-N linkage or C-H bending vibration due to capping agents. In fig(a) nickel oxide peak observed at 801.10 cm^{-1} and in fig (b) peaks observed in between $600-561.18\text{ cm}^{-1}$.

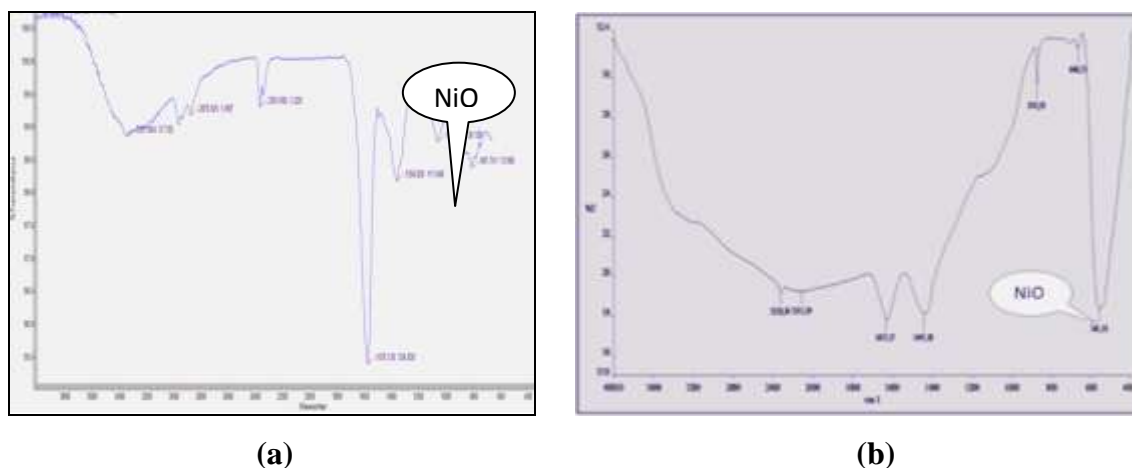


Fig. 2: FT-IR Spectra of prepared NiO nanoparticles. (a)TBAB and (b) TOAB at current density 10mA/cm^2

2] UV visible spectroscopic analysis

The reduction of nickel ions was visibly evident from the color changes associated with it. The optical spectra shows absorption bands in the range $360-370\text{nm}$ which confirms the metallic nature. These Ni nanoparticles are encapsulated with TBAB and TOAB which is completely removed only after calcinations. The increasing in intensity of the UV band and shifting to higher wavelength may be resulting due to presence of capping agent. As the electrochemical process is a function of current density, the formation of nanoparticles is diffusion controlled and it also depends on the concentration of ions at the electrode surface and in the bulk.

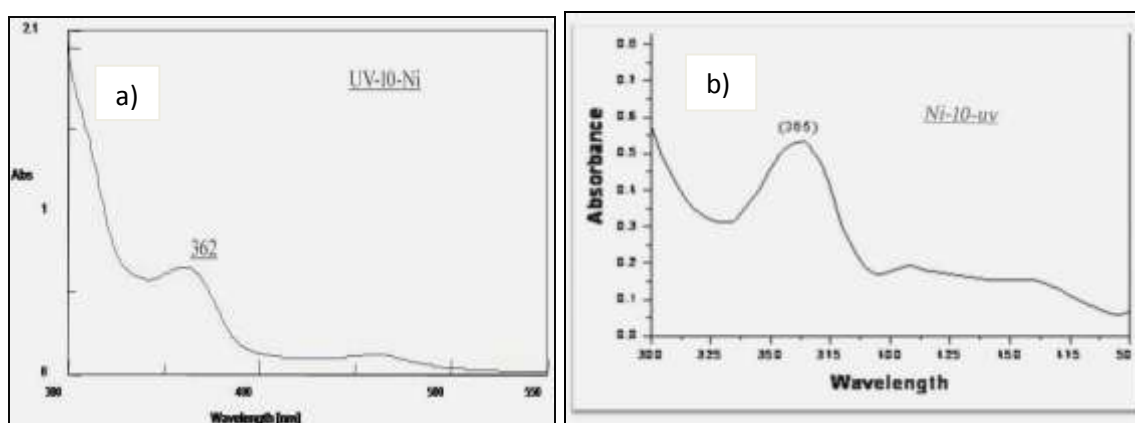


Fig. 3 Optical absorption spectrum for Ni nanoparticles (a) TBAB and (b) TOAB at current density 10mA/cm^2 .

3] XRD PATTERN

Estimation of crystallite size from X-ray diffraction

X-ray line broadening analysis provides a method of finding bulk average size of coherently diffracting domains. The average crystallite size (D) of solid material can be estimated from X-ray line broadening using the Debye-Scherrer equation.^[21-22]

$$D = \frac{K\lambda}{\beta \cos \theta}$$

Where, D = Average particle size, λ = wavelength, θ = diffraction angles, β = FWHM (Full width half maximum).

Particle size studies

X-ray diffraction (XRD) pattern of the prepared compound reveals the crystalline nature, phase purity and structure details. Figure 4(a) and (b) show the powder XRD pattern recorded for as prepared nickel oxide. The powder X-ray diffraction (XRD) with nickel filtered CuK α ($\lambda = 1.5405 \text{ \AA}$) radiation. Five diffraction peaks (111), (200), (220), (311) and (222) were observed, not only their peak position but their intensity also Matches the standard pattern of FCC type NiO with a space group of Fm $\bar{3}$ m(225) (Joint Committee on Powder Diffraction Standards (JCPDS) file no. 04-0835).^[23-24] The 2θ values for the planes (111), (200), (220), (311) and (222) were found to be 38.57, 44.5°, 51.94° 62.42° and 76.42° respectively.

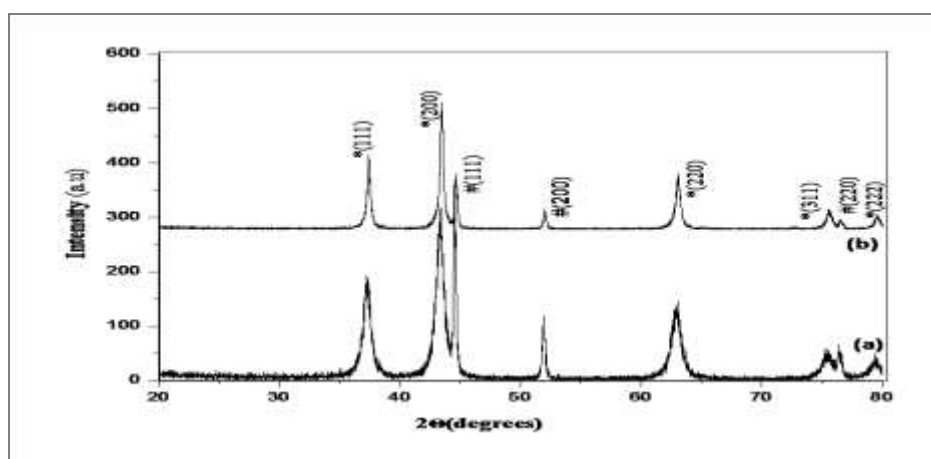


Figure 4: Shows X-ray diffraction pattern of prepared nickel nanoparticles. (a)TBAB (b) TOAB at 10mA/cm.²

The XRD pattern shows face centered cubic structure (FCC). No distinct diffraction peak other than those from FCC-Ni was found in the sample. The lattice constant is $a = b = c$ were

3.4392 Å, matched with JCPDS file no. 04-850 as shown in figure 4 (b). The broad diffraction peaks are due to nano-size of particles. Maximum intensity peak (111) was used to estimate the crystallite size and it is found to be 14-50 nm using Scherer equation. At the current density 10mA/cm² with TOAB Sharp peaks observed as compared with TBAB 10mA/cm².

Table: 1 –Average particle size of nickel oxide NPs.

Entry	Stabilizer	Phase	Average Size (nm)
1	TBAB	NiO	24.20
		Ni	40.24
2	TOAB	NiO	20.36
		Ni	36.26

4] SEM

Scanning electron (SEM) microscopy imaging technique was utilized to acquire information about the particle morphology on the nanoscale. Figure5: (a) TBAB at 10mA/cm² and (b) TOAB at 10mA/cm² show the low and high magnification images of NiO. The shape of the Ni particles are spherical and are linked together. The formation of particle aggregates were observed due to strong interaction among of nickel oxide nanoparticles. In the Fig. 5.a obtained at 10µm resolution which revealed that the Ni NPs were irregular polygonal, cylindrical and spherical in shape. The Fig. 5.b show a microgram at a resolution of 5µm. The microgram appears to be diffused and shows uneven morphology. Both SEM micrograph in Fig.5.a and b of the nickel nanoparticles shows the presence of porous nanoparticles that are agglomerated irregularly which might have been resulted from magnetic interaction and polymer adherence between the particles. Fig.5.b shows the presence of deep vacant space between the particles.

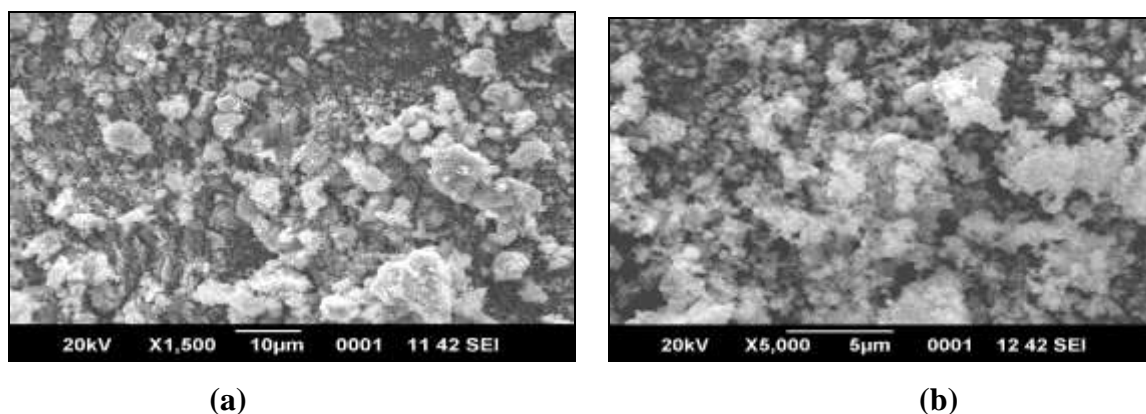


Figure 5: shows SEM image of nickel nanoparticles: 1500 and 5000 magnification with (a) TBAB (b) TOAB at 10mA/cm².

5] EDS

Energy-dispersive spectroscopic study confirmed the presence of nickel oxide with energy bands centered on 7.5 and 8.3 keV (K lines) and at 0.8 keV (L lines). The component oxygen showed in the graph is due to the capping agent attributed to partial oxidation of the nanoparticles during the handling of the sample due to atmospheric oxygen.

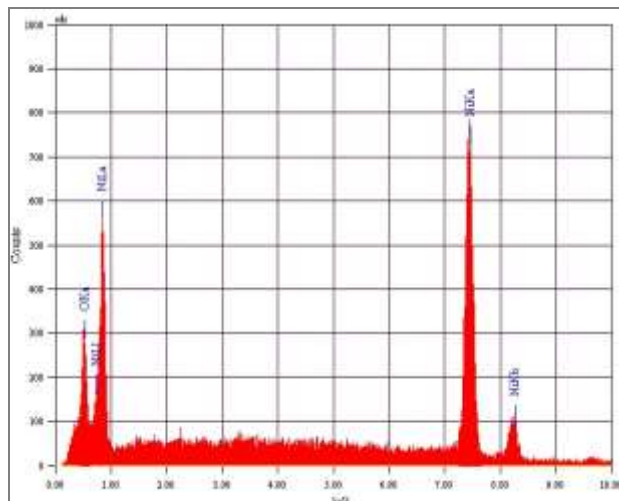


Fig 6: EDS spectrum of NiO nanoparticles and composition of elements.

Elements	Mass%	Atom%
Ni	96.05	88.96
O	3.95	11.04
Total	100	100

5] TEM

TEM analysis of nickel nanoparticles was carried out to study the variation of particle size as function of current density. Micrograph obtained from transmission electron microscope clearly indicated the decrease in particle size with increase in bulkiness capping agent, which resembled to the phenomenon observed in XRD pattern. Micrographs indicate that most particles were fine with various sizes, spherical, elongated and some clusters have also been observed in the Fig.7.a. and Fig.7.b. Figure also shows the aggregation of particles, their creation may be due to the influence of the interfacial energies and interparticle magnetic interactions. The appearance of some darker particles results from an enhanced diffraction contrast due to their orientation with respect to electron beam. The average particles size was measured to be 14-50 nm for 10mA/cm² current density with different capping agent, which was in good agreement with calculated particles size by XRD analysis.

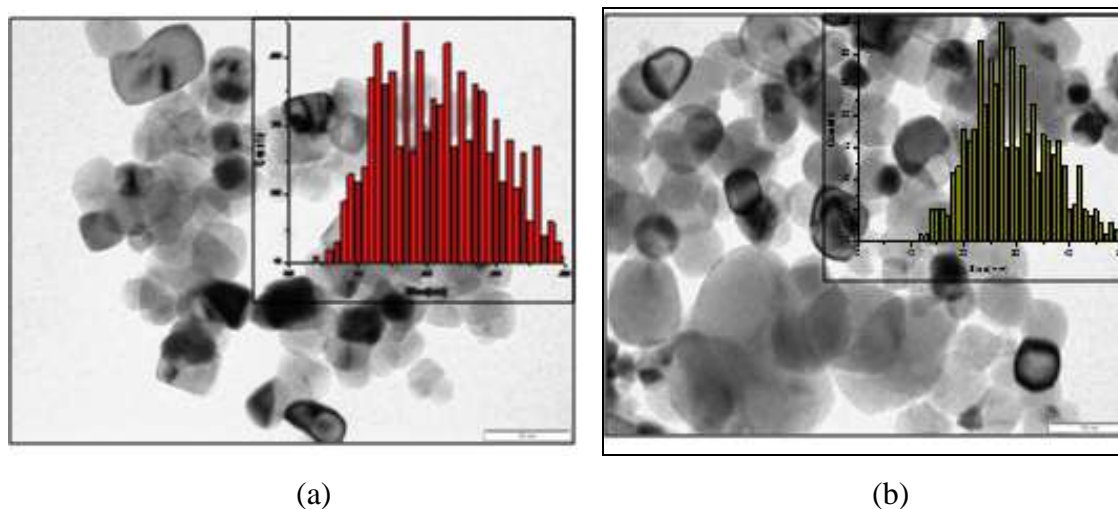


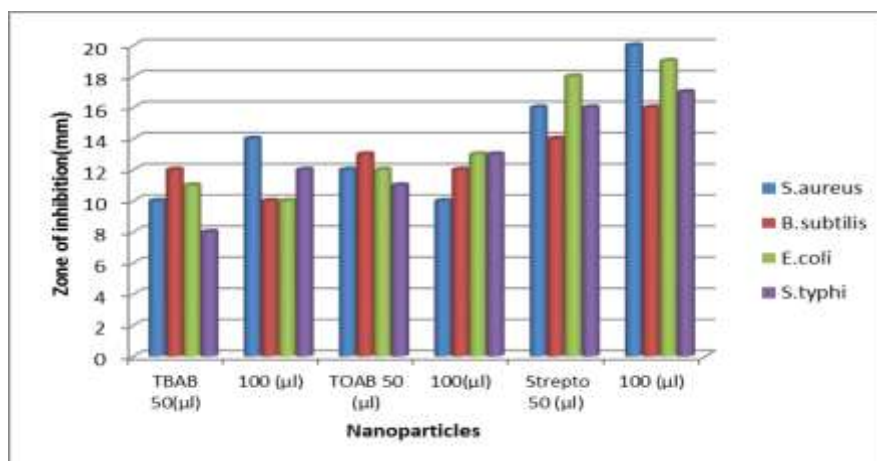
Figure 7: Shows TEM image of nickel nanoparticles and histogram at (a) TBAB (b) TOAB at 10mA/cm².

ANTIBACTERIAL ACTIVITY

The effect of fabricated Nickel nanoparticles have been checked against two gram positive bacteria *Bacillus subtilis* and *Staphylococcus aureus* and two gram negative bacteria *i.e.* *Escherichia coli* and *Salmonella typhi* by Kirby Baur's disc diffusion method, for two different concentrations of NiO nanoparticles *i.e.* 50 μ l, 100 μ l and compared with well known antibiotic Streptomycin. From the results in Table-2 it can be seen that all samples have better antimicrobial activity as all sample has zone of inhibition with size more than 9mm. The ACN/THF control did not show any antimicrobial activity against the tested bacterial strains. In addition, the antimicrobial activity is directly proportional to the nanoparticles concentration and 100 μ l is the optimum concentration of both nanoparticles for inhibiting growth of bacterial test organism. The structural difference of the cell wall plays an important role in tolerance or susceptibility of bacteria in the presence of NPs. The Gram-positive bacteria have a relatively thick wall composed of many layers of peptidoglycan polymer and only one membrane. In addition the outer membrane of the Gram-negative bacteria cells influences the permeability of many molecules.^[25-26]

Table:2- Antibacterial results of nickel Nps with different concentration and various microorganisms.

Entry	Metal	Stabilizer	Concentration	Antimicrobial activity Diameters of inhibition zone (mm)			
				Gram positive		Gram Negative	
				<i>S.aureus</i>	<i>B.subtilis</i>	<i>E.coli</i>	<i>S.typhi</i>
1	<i>Nickel</i>	TBAB	50(μ l)	10	12	11	08
2			100 (μ l)	14	10	10	12
3	<i>Nickel</i>	TOAB	50 (μ l)	12	13	12	11
4			100(μ l)	10	12	13	13
5	<i>ACN+THF(4:1)</i>		50 (μ l)	00	00	00	00
6			100 (μ l)	00	00	00	00
7	<i>Streptomycin</i>		50 (μ l)	16	14	18	16
8			100 (μ l)	20	16	19	17



Graph:1 Zone of inhibition in (mm) of nickel nanoparticles with different microorganisms.

CONCLUSION

We have successfully synthesized nickel nanoparticles by electrochemical reduction method with different stabilizers. The FTIR spectroscopic study of the Ni nanoparticles confirmed the removal of the capping agent after calcinations. The optical spectra show absorption bands in the range 360-370nm which confirm the metallic nature in both stabilizers. The XRD analysis of the different Ni nanoparticles showed the formation of Ni/NiO nanoparticles with face centered cubic structure and average particle size was found 14-50 nm both by using the capping agents. At the current density 10mA/cm² with TOAB sharp peaks were observed as compared to TBAB 10mA/cm². SEM confirms that the particles are in nano size and the appearances of particles are in irregular polygonal, and spherical. EDS analysis showed the formation of NiO nanoparticles. The TEM confirms that average particle size was 10-50 nm.

Nickel nanoparticles showed good antibacterial study with TOAB as compared with TBAB at different concentrations and various microorganisms.

ACKNOWLEDGEMENTS

The authors are grateful to Department of Chemistry, Dr. Babasaheb Ambedkar Marathwada University, Aurangabad and UGC-SAP-DRS-1 scheme New Delhi for providing laboratory facility. One of the authors (ASR) thankful for financial assistance from Major Research project University Grants Commission, New Delhi. The author (AAA) is also thankful to the University Grants Commission, New Delhi for Rajiv Gandhi National Fellowship.

REFERENCES

1. Ajeet Kumar¹, Amit Saxena¹, Arnab De², Ravi Shankar¹ and Subho Mozumdar, 1: 2001.
2. Kumar A, Kumar S, Saxena A, De A and Mozumdar S 2008 *Catal. Commun.*, 9: 778.
3. Knecht M R, Garcia-Martinez J C and Crooks R M 2006 *Chem. Mater.*, 18: 5039.
4. Patel J D, Canar O and Jones J 2007 *Pharm. Res.*, 24: 343.
5. Chen R Y and Zhou K G 2006 *Trans. Nonferr. Met. Soc. China*, 16: 1223.
6. Chen, D., Li, J., Shi, C., Du, X., Zhao, N., Sheng, J. and Liu, S., 2007. Properties of Core-Shell Ni-Au Nanoparticles Synthesized through a Redox-Transmetalation Method in Reverse Microemulsion, *Chemistry of Materials*, 19: 3399-3405.
7. Ozgur, O., Nahit, A., Erk, I., Nurettin, S., 2011. hydrogel assisted nickel nanoparticle synthesis and their use in hydrogen production from sodium boron hydride, *International Journal of Hydrogen Energy*, 36(3): 1998–2006.
8. Sun, C., Lee, J.S.H. and Zhang, M., 2008. Magnetic nanoparticles in MR imaging and Drug Delivery, *Advanced Drug Delivery Reviews*, 60.
9. D. B. Wang, C. X. Song, Z. S. Hu, X. Fu, *J. Phys. Chem. B*, 2005; 109: 1125.
10. Taherkhani, H. Karimi-Maleh, A.A. Ensafi, H. Beitollahi, A. Hosseini, M.A. Khalilzadeh, H. Bagheri, *Chin. Chem. Lett.*, 2012; 23: 237.
11. A.A. Ensafi, H. Karimi-Maleh, M. Keyvanfard, *Int. J. Env. Anal. Chem.* (2012) DOI:10.1080/03067319.2011.637198.
12. M.R. Akhgar, H. Beitollahi, M. Salari, H. Karimi-Maleh, H. Zamani, *Anal. Methods*, 2012; 4: 259.
13. H. Beitollahi, J.B. Raoof, H. Karimi-Maleh, R. Hosseinzadeh, *J. Solid State Electrochem.*, 2012; 16: 1701. 1252-1265.

14. Yoshio et al., 1998; Moon et al., 1995; Alcantara et al., 1998; Wu et al., 2008; Miller and Rocheleau, 1997; Gabr et al., 1992.
15. Priyanka L. Anandgaonkar, Sunita Jadhav, Suresh T. Gaikwad, Anjali S. Rajbhoj, *Journal of Cluster Science*, 2014; 25: 483-493.
16. Izaki Y, Mugikura Y, Watanabe T, Kawase M, Selman JR. Direct observation of the oxidation nickel in molten carbonate. *J Power Sources*, 1998; 75(2): 236-43.
17. Ichiyanagi Y, Wakabayashi N, Yamazaki J, Yamada S, Kimishima Y, Komatsu E, et al. Magnetic properties of NiO nanoparticles. *Phys. B.*, 2003; 329-333: 862-3.
18. Hotovy I, Huran J, Spiess L, Hascik S, Rehacek V. Preparation of nickel oxide thin films for gas sensors applications. *Sens Actuators. B.*, 1999; 57(1-3): 147-52.
19. Biju V, Khadar MA. Fourier transform infrared spectroscopy study of nanostructured nickel oxide. *Spectrochim Acta Part A.*, 2003; 59(1): 121-34.
20. Reetz M.T., Helbig W., Quaiser S.A., in *Active metals VCH: Weinheim*, 1996; 279.
21. Reetz M.T., Breinbauer R., Wanninger K., *Tetrahedron Lett.*, 1996; 37: 4499.
22. Scherrer P., *Göttinger Nachrichten Gesell.*, 1918; 2: 98.
23. P Christophe; L Patricia; P Marie-Paule. *J. Phys. Chem.*, 1993; 97: 12974.
24. Nowsath Rifaya M., Theivasanthi T., Alagar M., *Nanoscience and Nanotechnology*, 2012; 2(5): 134-138.
25. Mani Rahulana K., Padmanathanb N., Reji Philip, Balamurugand S., Kanakam C.C., *Appl. Surface Sci.*, 2013; 282: 656-661.
26. Tortora G, Funke R.B., Case L.C. *Microbiology: an introduction*. Addison-Wesley Longman Inc, New York, 2001.